Original Article
Basic Research

Diabetes Metab J 2023;47:287-300
https://doi.org/10.4093/dmj.2021.0306
pISSN 2233-6079 · eISSN 2233-6087

dmj
DIABETES & METABOLISM JOURNAL

N^6-Methyladenosine Methyltransferase METTL3 Alleviates Diabetes-Induced Testicular Damage through Modulating TUG1/Clusterin Axis

Yuan Tian[1], Yue-Hai Xiao[1], Chao Sun[2], Bei Liu[1], Fa Sun[2]

[1]Department of Urology, Affiliated Hospital of Guizhou Medical University, Guiyang,
[2]School of Clinical Medicine, Guizhou Medical University, Guiyang, China

Background: The present study investigated the regulatory effects of N^6-methyladenosine (m6A) methyltransferase like-3 (METTL3) in diabetes-induced testicular damage.
Methods: *In vivo* diabetic mice and high glucose (HG) treated GC-1 spg cells were established. The mRNA and protein expressions were determined by real-time quantitative polymerase chain reaction, Western blot, immunofluorescence and immunohistochemistry staining. Levels of testosterone, blood glucose, cell viability, and apoptosis were detected by enzyme-linked immunosorbent assay, MTT, and flow cytometry, respectively. Molecular interactions were verified by RNA immunoprecipitation and RNA pull-down assay. Histopathological staining was performed to evaluate testicular injury.
Results: METTL3 and long non-coding RNA taurine up-regulated 1 (lncRNA TUG1) were downregulated in testicular tissues of diabetic mice and HG-treated GC-1 spg cells. METTL3 overexpression could reduce the blood glucose level, oxidative stress and testicular damage but enhance testosterone secretion in diabetic mouse model and HG-stimulated GC-1 spg cells. Mechanically, METTL3-mediated m6A methylation enhanced the stability of TUG1, then stabilizing the clusterin mRNA via recruiting serine and arginine rich splicing factor 1. Moreover, inhibition of TUG1/clusterin signaling markedly reversed the protective impacts of METTL3 overexpression on HG-stimulated GC-1 spg cells.
Conclusion: This study demonstrated that METTL3 ameliorated diabetes-induced testicular damage by upregulating the TUG1/clusterin signaling. These data further elucidate the potential regulatory mechanisms of m6A modification on diabetes-induced testicular injury.

Keywords: Apoptosis; Clusterin; Diabetes mellitus; Methylation; Oxidative stress; RNA, long noncoding

INTRODUCTION

Diabetes-induced testicular damage (DITD) is a prevalent complication of diabetes mellitus characterized by increased spermatogenic cell apoptosis, low sperm levels and motility, and dysregulated testicular endocrine function [1]. Approximately 90% of male patients with diabetes experience varying degrees of testicular dysfunction [2]. Moreover, the incidence of sexual dysfunction and infertility in patients with diabetes is about 10 times higher relative to the non-diabetic population [3]. Previous evidence suggests that excessive oxidative stress during diabetes can impair testicular microcirculation and spermatogenesis [4]. However, the exact mechanisms of DITD remain largely unclear.

N^6-methyladenosine (m6A) modification is the most abundant post-transcriptional modification in RNA production and metabolism [5]. m6A modification is a dynamic process that can be recognized by binding proteins ("readers"), medi-

Corresponding author: Fa Sun https://orcid.org/0000-0002-0841-4668
School of Clinical Medicine, Guizhou Medical University, No. 9 Beijing Road, Yunyan District, Guiyang 550004, Guizhou Province, China
E-mail: sunfa8526@163.com

Received: Nov. 2, 2021; Accepted: Jun. 29, 2022

ated by methyltransferases ("writers"), and then removed by demethylases ("erasers") [6]. Methyltransferase like-3 (METTL3) is a major methyltransferase responsible for m6A modification and the stability of targeted mRNAs [7]. Accumulating researches referenced that METTL3-mediated m6A modification is involved in diabetes and its complications. For instance, Yang et al. [8] reported that silencing of METTL3 facilitated the proliferation but repressed apoptosis in high glucose (HG)-stimulated lens epithelial cells by stabilizing intercellular adhesion molecule-1. Zha et al. [9] found that METTL3 was downregulated in diabetes mellitus patients, and overexpression of METTL3 protected retinal pigment epithelium (RPE) cells from HG induced cytotoxic effects via activating m6A-mediated long non-coding RNA (lncRNA) DGCR8 microprocessor complex subunit (DGCR8). These evidences suggested that the roles and underlying mechanism of METTL3 in DITD is worth to investigated.

lncRNAs, a subtype of non-coding RNAs with >200 nucleotides in length, which play an important role in diabetes and its complications. For instance, lncRNA metastasis associated lung adenocarcinoma transcript 1 (MALAT1) was overexpressed in diabetic rats, and silencing of MALAT1 relieved diabetic retinopathy by affecting the proliferation, migration, and tube formation of RPE cells [10]. Yang et al. [11] proved that lncRNA KCNQ1 opposite strand/antisense transcript 1 (KCNQ1OT1) downregulation inhibited pyroptosis in diabetic cardiomyopathy by regulating miR-214-3p and caspase-1. In addition, lncRNA taurine up-regulated 1 (TUG1) also plays a vital regulatory role in diabetes and related complications [12]. The upregulation of TUG1 improved the function of endothelial progenitor cells in HG conditions by promoting cell proliferation, migration and tube formation *in vitro* [13]. These findings indicated that the potential role of TUG1 in DITD warrants exploration.

Clusterin is a secreted chaperone activated by stress that can regulate a series of pathological processes [14]. In general, clusterin frequently acts as a protective factor in diabetes. Ren et al. [15] revealed that clusterin could downregulate proinflammatory cytokines and suppressed monocyte adhesion to endothelial cells in diabetes via attenuating mitochondrial fragmentation. Clusterin was elevated in diabetic nephropathy and inhibited apoptosis of podocytes [16]. Importantly, clusterin was downregulated in testis tissues of diabetic rats, and upregulation of clusterin could rescue cell viability and inhibited cell apoptosis in HG-treated GC-1 spg cells via regulating phosphoinositide 3-kinase (PI3K)/AKT/mammalian target of rapamycin (mTOR) signaling [17]. Accordingly, elucidating the upstream regulatory mechanism of clusterin maybe help us better understand the mechanism of DTID.

GC-1 spg cell line is a commercially available germ cell line that represents the period between primary spermatocytes of type B spermatogonia [18]. Recently, GC-1 spg cells were widely used to establish *in vitro* model of diabetes-induced testicular injury [17,19]. In the present study, we explored the potential regulatory effects of METTL3 on DITD using a mouse model of streptozocin (STZ)-induced diabetes and HG-treated mouse GC-1 spg cells. Our findings would further elucidate the pathological mechanisms of DITD.

METHODS

Adenovirus overexpression

pcDNA3.1-METTL3 and empty pcDNA3.1 vector were purchased from GenePharma (Shanghai, China). By referring to the previously described [20], the recombinant METTL3 overexpressing adenovirus vector were established. In brief, the full length of METTL3 was cut off from pcDNA3.1-METTL3 vector between Hind III and Xhol restriction endonuclease sites, and then connected to the pENTR1A-expressing vector (Life Technologies, Carlsbad, CA, USA) to construct pENTR1A-METTL3. After the LR reaction a recombination reaction between attL and attR sites using LR Clonase II enzyme mix, the pENTR1A-METTL3 and pAd/CMV/V5-DEST (ThermoFisher Scientific, Carlsbad, CA, USA) was recombined to form pAd/CMV/V5-DEST-METTL3 (pAd-METTL3). The recombined pAd-METTL3 were transfected into 293T cells to obtain purified virus particles.

Animal model

C57BL/6 mice (6-week-old) were obtained from the Laboratory Animal Unit. The experimental protocols were approved by the Experimental Animal Committee of Guizhou Medical University (No.1900647). Then, mice were randomly divided into two groups: control ($n=20$) and STZ ($n=40$). The model of STZ-induced diabetes was established by intraperitoneally injecting mice with STZ (45 mg/kg body weight; Sigma-Aldrich, St. Louis, MO, USA) for 5 successive days. Animals in the control group were administered with normal saline. The fasting blood glucose of mice following STZ injection was measured once a week. The diabetic model was considered

successfully established when the fasting glucose level was greater than 16.7 mmol/L.

STZ-induced diabetic mice were further divided into three groups: STZ, STZ+pcDNA3.1, and STZ+METTL3. Animals in the STZ+METTL3 group were intravenously injected with pAd-METTL3 vectors (10^9 plaque forming unit per mouse), while those in the STZ+pcDNA3.1 group were injected with pAd-NC vectors (10^9 plaque forming unit per mouse). The STZ group was administered with phosphate-buffered saline following the same procedure. After another 4 weeks, all mice were euthanized. Their serum and testicular tissues were collected for further analysis.

Detection of blood glucose level

After the mice fasted for 12 hours, blood samples were collected and blood glucose concentration was measured with a glucometer (ACCU-CHECK Compact Plus, Roche Diagnostics, Switzerland).

Cell culture and transfection

Mouse spermatogenic GC-1 spg cell line was purchased from the American Tissue Culture Collection (Shanghai, China) and cultured in Dulbecco's Modified Eagle Medium (DMEM, Invitrogen, Waltham, MA, USA) containing 10% fatal bovine serum (Invitrogen) at 37°C with 5% CO_2. To establish a DITD model *in vitro*, GC-1 spg cells were stimulated by 30 mmol/L of glucose (Invitrogen) for 24 hours. Small interfering (si) RNAs targeting METTL3 (si-METTL3), serine and arginine rich splicing factor 1 (SRSF1; si-SRSF1), pcDNA3.1-METTL3, pcDNA3.1-TUG1, and corresponding scrambled controls were purchased from GenePharma. Target plasmid vectors or negative controls were transfected to GC-1 spg cells using Lipofectamine 3000 (Invitrogen).

RNA stability assay

After indicated treatment, cells were incubated with actinomycin D (5 μg/mL) (Sigma-Aldrich) for 0, 2, 4, and 6 hours. Then, cells were harvested and the RNA remaining was quantified by real-time quantitative polymerase chain reaction (RT-qPCR).

MTT assay

After indicated treatment, the mixture was discarded and cells were washed by PBS. 10 μL MTT solution were added in each well for incubation for 4 hours. Afterwards, 150 μL dimethyl sulfoxide was added and shacking for 10 minutes at low speed to dissolve the crystal. Finally, the absorbance was measured at 490 nm.

Enzyme-linked immunosorbent assay

The level of testosterone in cell supernatant or serum samples was measured by enzyme-linked immunosorbent assay (ELISA) kit (CUSABIO, Wuhan, China) following the instructions. The optical density of each sample was detected at 450 nm.

Oxidative stress detections

The intracellular reactive oxygen species (ROS) level were detected using the 2′,7′-dichlorodihydro-fluorescin diacetate (DCFH-DA, Beyotime Biotechnology Inc., Haimen, China) probe as previously described [21]. Briefly, cells were washed with serum-free culture medium and incubated with 10 μM DCFH-DA for 30 minutes at 37°C. Then, cells were washed twice with serum-free culture medium. The fluorescence of 2′,7′-dichlorofluorescein was monitored using a fluorescence microscope (Olympus, Tokyo, Japan). The contents of malondialdehyde (MDA) and glutathione (GSH), and the activities of superoxide dismutase (SOD) and glutathione peroxidase (GSH-Px) in cells and mouse testicular tissues were detected by commercially available kits (Nanjing Institute of Bioengineering, Nanjing, China) accordingly to the manufacturer's protocols.

Apoptosis analysis

GC-1 spg cells were harvested and resuspended in binding buffer to a density of 5×10^6 cells/mL. fluorescein isothiocyanate (FITC) Annexin V apoptosis detection kit (BD Biosciences, Franklin Lakes, NJ, USA) was used for cell apoptosis assay. Each sample was added with a mixture of 5 μL FITC-Annexin V and 5 μL propidium iodide and incubated in the dark for 20 minutes. The fluorescence emission was detected by flow cytometry and apoptosis was analyzed using the FlowJo software v10.0.

Immunohistochemistry

The paraffin-embedded sections (4 μm) were dewaxed, blocked with serum for 1 hour, and then stained with anti-METTL3 antibody (cat# ab195352, Abcam, Cambridge, UK) for 2 hours. Subsequently, sections were incubated with a goat anti-rabbit immunoglobulin G (IgG)/horseradish peroxidase (HRP) antibody for 30 minutes and stained with the diaminobenzidine (DAB) solution.

Immunofluorescence staining

After indicated treatment, cells were fixed, blocked with bull serum albumin, and then incubated with goat anti-rabbit IgG Alexa Fluor (cat# 150077, Abcam) for 1 hour. 4′,6-Diamidino-2-phenylindole (DAPI, Sigma-Aldrich) was used for nuclear staining. The expression of METTL3 was analyzed by fluorescence microscopy (Olympus).

TUNEL assay

The apoptotic rate of cells in testicular tissues collected from diabetic mice was examined by terminal deoxynucleotidyl transferase dUTP nick end labeling (TUNEL) Detection Kit (Thermo Fisher Scientific, Waltham, MA, USA). First, terminal deoxynucleotidyl transferase (TdT) reagent and dUTP reagent were mixed proportionally to prepare the working solution. Before analysis, tissue sections (4 μm) were dewaxed, permeabilized, and incubated with the working solution at 37°C for 2 hours. Sections were then washed with PBS and incubated with hydrogen peroxide solution for 15 minutes. After decolorization, sections were treated with converter-POD reagent for 30 minutes, followed by the DAB solution, and finally by hematoxylin dye for nuclear staining. Apoptosis was examined under a fluorescence microscope (Olympus).

Hematoxylin and eosin (H&E) staining

Testicular tissue sections from diabetic mice were dewaxed and stained with H&E (Solarbio, Beijing, China) for nuclear and cytoplasm staining, respectively. Then, the remaining dye was washed. The slides were dehydrated and observed under a microscope.

RT-qPCR

Total RNA was extracted by TRIzol reagent (Invitrogen) and reserved transcribed into cDNA using the PrimScript kit (Takara Biotechnology, Beijing, China). Then, RT-qPCR was performed using 7500 Fast & 7500 Real-Time PCR System (ThermoFisher Scientific) and SYBR Green PCR Master Mix (ThermoFisher Scientific). The relative gene expression was calculated by the $2^{-\Delta\Delta Ct}$ method and glyceraldehyde-3-phosphate dehydrogenase was the internal control. The primers were listed in Table 1.

Table 1. Real-time quantitative polymerase chain reaction primer sequences

Gene	Sequences
METTL3	(F) 5′-AGCCTTCTGAACCAACAGTCC-3′
	(R) 5′-CCGACCTCGAGAGCGAAAT-3′
TUG1	(F) 5′-TAGCAGTTCCCCAATCCTTG-3′
	(R) 5′-CACAAATTCCCATCATTCCC-3′
Clusterin	(F) 5′-CGGAAGTGTGTAACGAGACCA-3′
	(R) 5′-ATCTTCAGGCATCCTGTGGAG-3
GAPDH	(F) 5′-ATGCTGGCGCTGAGTACGTC-3′
	(R) 5′-CAGGGGTGCTAAGCAGTTGGT-3′

METTL3, methyltransferase like-3; TUG1, taurine up-regulated 1; GAPDH, glyceraldehyde-3-phosphate dehydrogenase.

Western blot

The total proteins were extracted by radio immunoprecipitation assay (RIPA) reagent and quantified by bicinchoninic acid assay (BCA) assay (Bio-Rad, Hercules, CA, USA), the samples were separated by 10% sodium dodecyl sulfate-polyacrylamide gel electrophoresis (SDS-PAGE) and then transfected onto the polyvinylidene fluoride (PVDF) membrane (Thermo Fisher Scientific). After blocking, PVDF membrane was incubated with specific antibodies overnight, including METTL3 (cat# ab195352, Abcam), Bcl-2 (cat# ab32124, Abcam), Bax (cat# ab3191, Abcam), cleaved caspase-3 (cat# ab32499, Abcam), cleaved caspase-9 (cat# ab32539, Abcam), and clusterin (cat# ab269342, Abcam) at 4°C. Subsequently, the membrane was incubated with goat anti-rabbit/mouse IgG (Abcam). Protein bands were visualized by ECL Western Blotting Substrate Kit (Abcam) and the intensity was determined by Image J.

RNA immunoprecipitation

Protein-A/G beads (Thermo Fisher Scientific) were resuspended by NT-2 buffer and incubated with anti-METTL3 (cat# ab195352, Abcam), anti-SRSF1 (cat# 32-4500, Thermo Fisher Scientific), anti-m6A (cat# ab208577, Abcam) antibodies at room temperature for 2 hours. Then, 100 μL cell lysates and 900 μL NET-2 (NET-2 buffer was consists of NT-2 buffer, EDTA, and DTT regents) buffer were added to eppendorf (EP) tubes containing Protein-A/G beads. The mixture was rotated and incubated overnight at 4°C. The immunoprecipitation was collected and purified by proteinase K and the expression of RNA was analyzed by RT-qPCR.

RNA pull-down assay

Pierce RNA 3′-End Desthiobiotinylation Kit (Thermo Fisher Scientific) was prepared for desthiobiotin labeling of TUG1

RNA. Biotin-labeled TUG1 RNA was kept at –80°C. Streptavidin magnetic beads (Thermo Fisher Scientific) were incubated with biotin-labeled TUG1 in binding buffer for 12 hours. Then, beads were incubated with cell lysates. The RNA-protein complex was examined by Western blot.

Statistical analysis

All experiments were performed in triplicate and data were presented as the mean values±standard deviation. Student *t*-test or one-way analysis of variance (ANOVA) for unpaired data was used to compare the values between two groups or among multiple groups, respectively. $P<0.05$ was considered statistically significant.

RESULTS

METTL3 and TUG1 were downregulated in diabetic mice

We first established a mouse model of STZ-induced diabetes to identify the expression patterns of METTL3 and TUG1. As shown in Fig. 1A, STZ treatment significantly increased the blood glucose levels of mice (>16.7 mmol/L) compared with the control group, indicating that the diabetic mouse model was successfully established. Moreover, the serum level of testosterone was notably decreased in mice injected with STZ

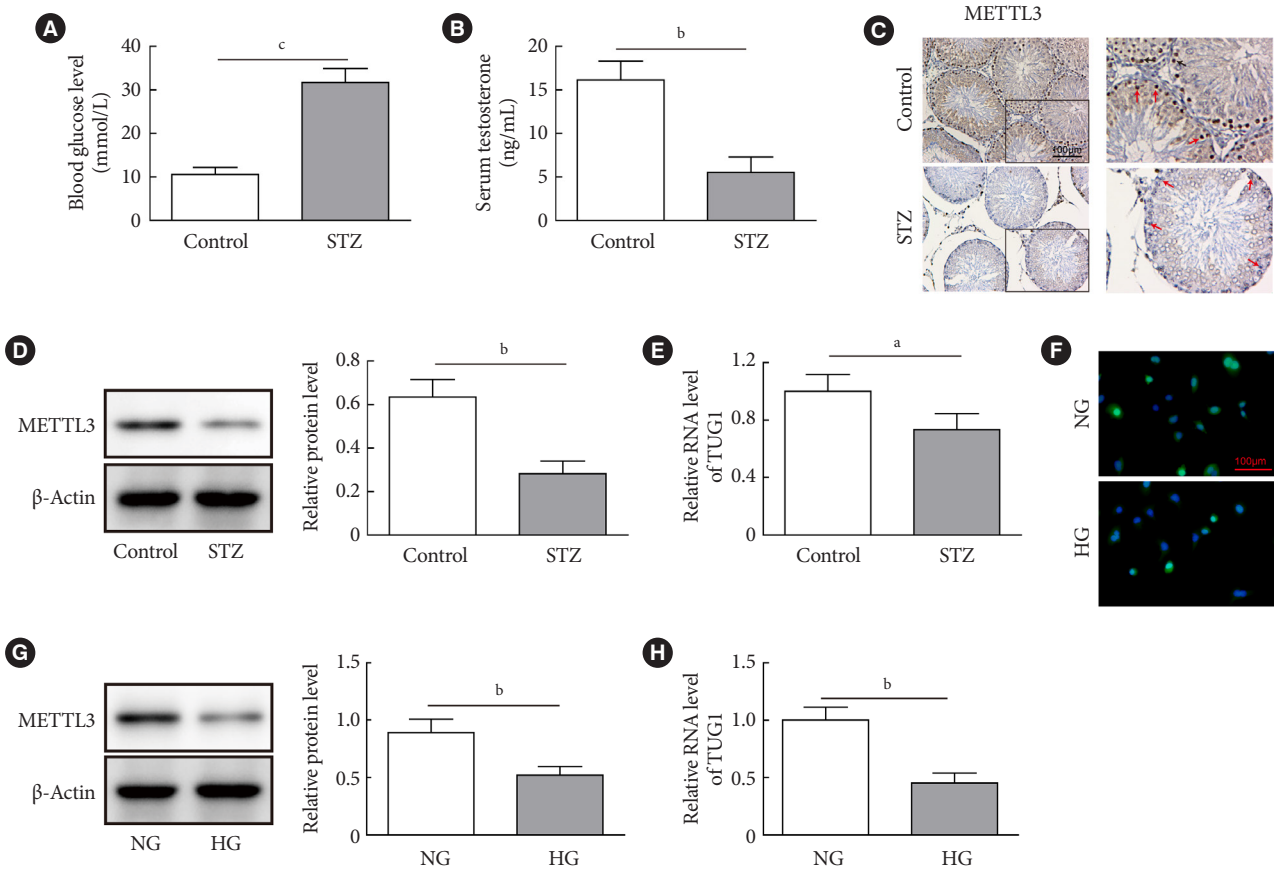

Fig. 1. Expressions of methyltransferase like-3 (METTL3) and taurine up-regulated 1 (TUG1) in diabetic mice. (A-D) C57BL/6 mice ($n=10$ per group) were injected with streptozocin (STZ) at a dosage of 45 mg/kg body weight for 5 days (the STZ group) or normal saline (the control group). (A) The blood glucose levels of STZ-treated mice and control mice were measured using a glucometer. (B) The serum level of testosterone was determined by enzyme-linked immunosorbent assay (ELISA). The testicular expression of METTL3 in mice was measured by (C) immunohistochemistry staining and (D) Western blot. (E) The expression of TUG1 was determined by real-time quantitative polymerase chain reaction (RT-qPCR). (F-H) Mouse spermatogenic GC-1 spg cells were cultured in Dulbecco's Modified Eagle Medium (DMEM) supplemented with 30 mmol/L of glucose for 24 hours. The expression of METTL3 was determined by (F) immunofluorescence staining and (G) Western blot. (H) The expression of TUG1 was determined by RT-qPCR. NG, normal glucose; HG, high glucose. $^{a}P<0.05$, $^{b}P<0.01$, $^{c}P<0.001$.

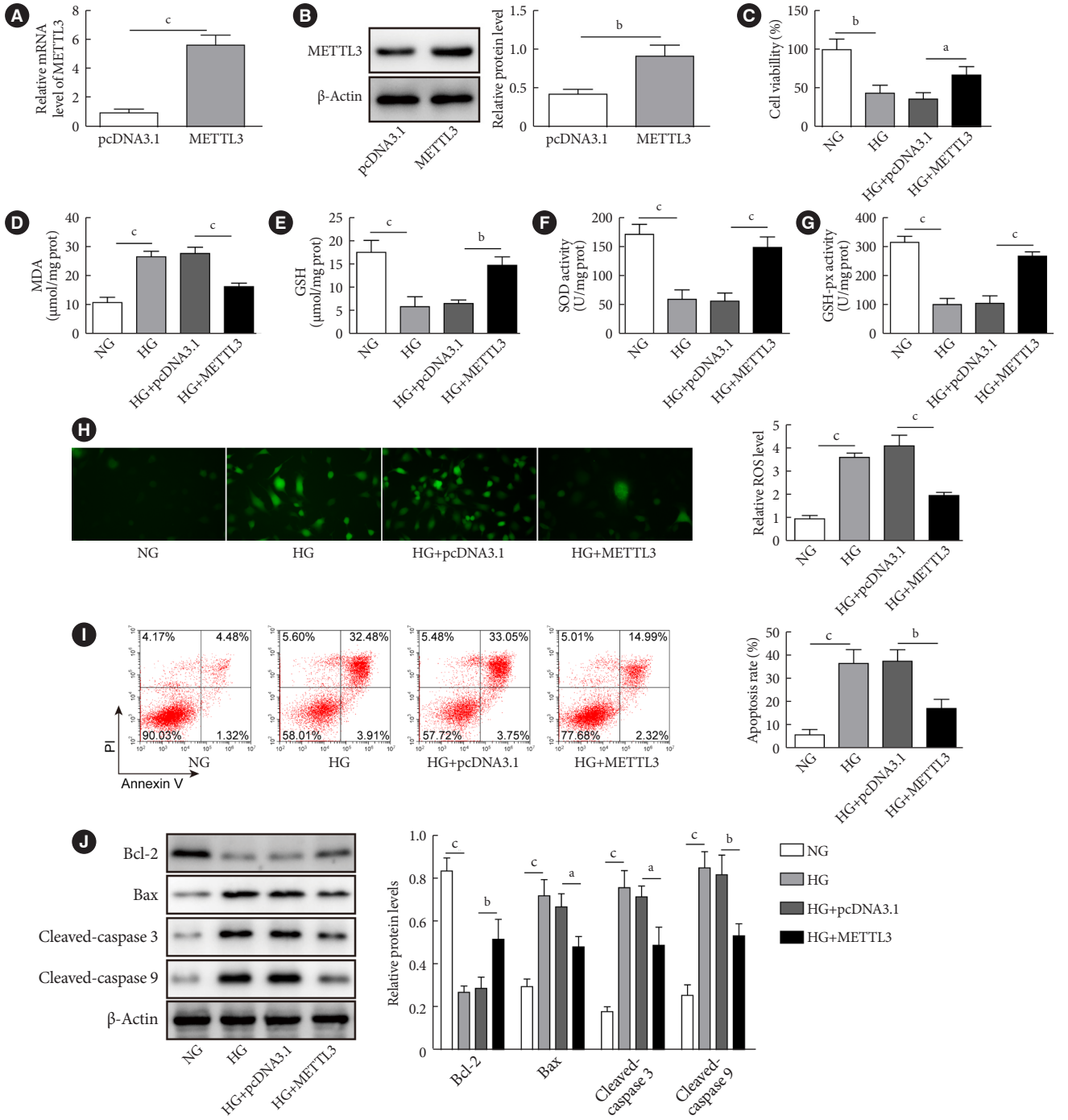

Fig. 2. Effects of methyltransferase like-3 (METTL3) overexpression on the viability and apoptosis of GC-1 spg cells induced by high glucose. Mouse GC-1 spg cells were transfected with or without vectors overexpressing METTL3 or empty control vectors (pcDNA3.1), then cells were cultured in high glucose (HG) medium (30 mmol/L) for 24 hours. The expression of METTL3 in GC-1 spg cells was measured by (A) real-time quantitative polymerase chain reaction and (B) Western blot. (C) Cell viability was evaluated by the MTT assay. (D-H) The levels of malondialdehyde (MDA) and glutathione (GSH) and the activities of superoxide dismutase (SOD) and glutathione peroxidase (GSH-Px) in GC-1 spg cells treated with or without HG were measured by commercial kits. (H) The level of reactive oxygen species (ROS) was detected using the 2′,7′-dichlorodihydro-fluorescin diacetate (DCFH-AD) probe. (I) Cell apoptosis was determined by flow cytometry. (J) The expressions of Bcl-2, Bax, cleaved caspase-3, and cleaved caspase-9 were quantified by Western blot. NG, normal glucose. [a]$P<0.05$, [b]$P<0.01$, [c]$P<0.001$.

compared to the control group (Fig. 1B). Immunohistochemistry and Western blot analysis revealed that METTL3 in testicular tissues was dramatically downregulated in diabetic mice (Fig. 1C and D). Additionally, TUG1 was significantly downregulated in the testicular tissues of diabetic mice (Fig. 1E). Consistently, we also found that both METTL3 and TUG1 were markedly decreased in HG-administrated GC-1 spg cell model *in vitro* (Fig. 1F-H). These results demonstrated that METTL3 and TUG1 were downregulated in both diabetic mice and HG-cultured GC-1 spg cells.

METTL3 overexpression increased viability but reduced apoptosis of HG-treated GC-1 spg cells

To investigate the functional significance of METTL3 in DITD, we transfected GC-1 spg cells with METTL3 overexpressing vectors. As shown in Fig. 2A and B, METTL3 was substantially upregulated after transfection with pcDNA3.1-METTL3 vectors. MTT assay showed that the viability of GC-1 spg cells was reduced by HG stimulation, but recovered by METTL3 upregulation (Fig. 2C). Moreover, HG-treatment greatly increased the MDA and ROS levels but decreased GSH, SDH, and GSH-Px activities in GC-1 spg cells, while METTL3 overexpression effectively reversed these effects (Fig. 2D-H). The apoptosis induced by HG treatment was also attenuated by METTL3 overexpression (Fig. 2I). Consistently, HG treatment increased the protein expressions of Bax, cleaved caspase-3, and cleaved caspase-9, but downregulated Bcl-2; however, these expression patterns were dramatically reversed by METTL3 overexpression (Fig. 2J). Collectively, METTL3 overexpression increased viability and reduced apoptosis of HG-treated GC-1 spg cells.

METTL3-mediated m6A modification increased the stability of TUG1

We next investigate the mechanisms by which METTL3 regulated the viability and apoptosis of HG-treated GC-1 spg cells. RMVar (http://rmvar.renlab.org/) predicted an m6A modification site of METTL3 in TUG1 (Fig. 3A). Subsequent RNA immunoprecipitation (RIP) assay verified that TUG1 was enriched in the RNA complex pulled down by the anti-METTL3, rather than the anti-METTL14, anti-Wilms tumor 1-associated protein (WTAP), anti-fat mass and obesity-associated protein (FTO), or anti-alkB homolog 5 (ALKBH5) antibodies (Fig. 3B).

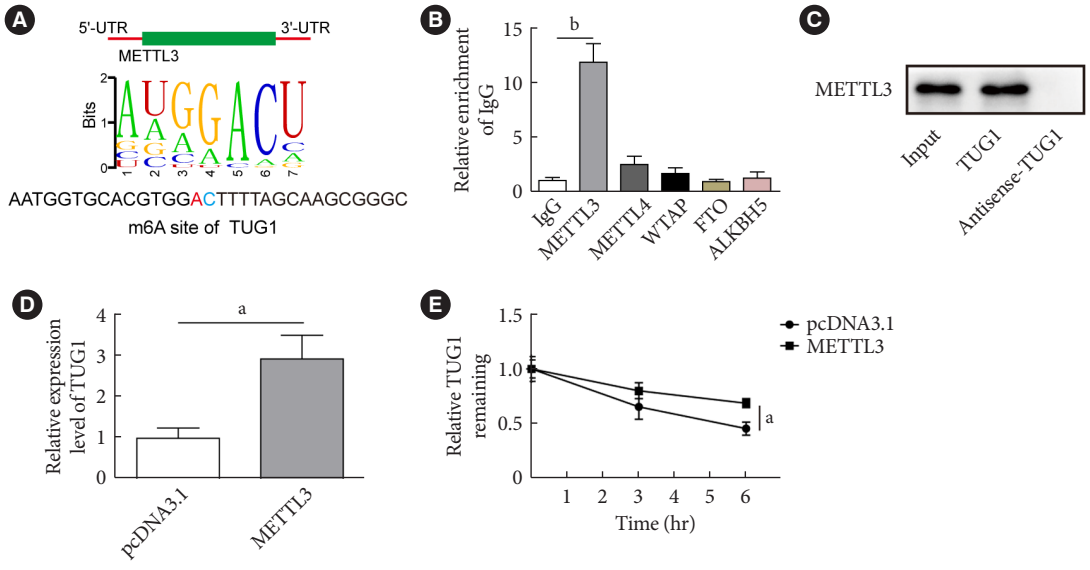

Fig. 3. Methyltransferase like-3 (METTL3)-mediated N^6-methyladenosine (m6A) modification increased the stability of taurine up-regulated 1 (TUG1) in high glucose (HG)-induced GC-1 spg cells. (A) The m6A site in TUG1 was predicted by RMVar (http://rmvar.renlab.org/). (B) RNA immunoprecipitation (RIP) was performed to verify the enrichment of TUG1 by METTL3. (C) RNA pull-down was used to validate the binding between METTL3 and TUG1. (D, E) GC-1 spg cells were transfected with vectors overexpressing METTL3 or control vectors. (D) The expression of TUG1 was measured by real-time quantitative polymerase chain reaction. (E) The half-life of TUG1 was determined by RNA stability assay. UTR, untranslated region; IgG, immunoglobulin G; WTAP, wilms tumor 1-associated protein; FTO, fat mass and obesity-associated protein; ALKBH5, alkB homolog 5. $^{a}P<0.01$, $^{b}P<0.001$.

Consistently, a direct binding relationship was identified in the RNA pull-down assay (Fig. 3C). In addition, the RNA expression of TUG1 was significantly elevated in cells transfected vectors overexpressing METTL3 in comparison with those transfected with pcDNA3.1 (Fig. 3D). The upregulation of METTL3 also attenuated the RNA degradative rate of TUG1 (Fig. 3E).

TUG1 increased the stability of clusterin mRNA by interacting with SRSF1

Through bioinformatics analysis, it was found that both TUG1 and clusterin might interact with SRSF1. To verify this finding, RIP and RNA pull-down detections were conducted and validated the interaction between SRSF1 and TUG1 (Fig. 4A and B). Next, we silenced SRSF1 in GC-1 spg cells by transfecting si-SRSF1. As shown in Fig. 4C, si-SRSF1 transfection notably reduced the mRNA expressions of SRSF1 and clusterin. Importantly, overexpression of TUG1 increased the mRNA level of clusterin, but this effect was suppressed by SRSF1 knockdown (Fig. 4D). RIP assay illustrated that TUG1 overexpression enhanced the abundance of clusterin in complex pulled down by anti-SRSF1 (Fig. 4E). Additionally, the upregulation of TUG1 enhanced the stability of the clusterin mRNA, but this effect was abolished by SRSF1 knockdown (Fig. 4F). These findings implied that TUG1 increased the stability of the clusterin mRNA via recruiting SRSF1.

TUG1/clusterin axis was involved in the regulation of HG-stimulated GC-1 spg cells by METTL3

This section was aimed to explore whether the TUG1/clusterin axis had a functional connection with METTL3 in HG-induced GC-1 spg cells. As shown in Fig. 5A and B, overexpression of METTL3 increased the RNA levels of TUG1 and clusterin in HG-stimulated GC-1 spg cells, but these trends were markedly abolished by transfection with si-TUG1. The promoting effects of METTL3 overexpression on the cell viability was diminished by TUG1 knockdown (Fig. 5C). Moreover, METTL3 overexpression reduced MDA and ROS levels and increased the activities of SOD, GSH, and GSH-Px in HG-treated GC-1 spg cells; however, these impacts were diminished by TUG1 knockdown (Fig. 5D-H). Similarly, TUG1

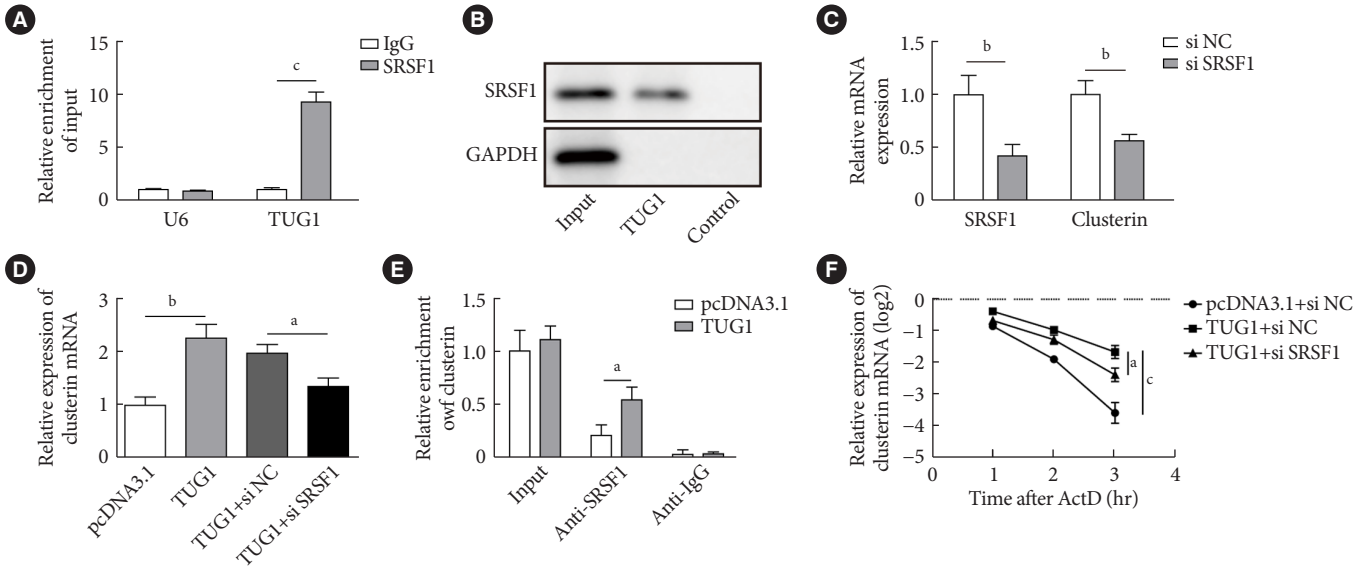

Fig. 4. Taurine up-regulated 1 (TUG1) increased the stability of clusterin mRNA by interacting with serine and arginine rich splicing factor 1 (SRSF1). (A) RNA immunoprecipitation (RIP) was performed to verify the enrichment of TUG1 by SRSF1. (B) RNA pull-down assay was used to validate the binding between SRSF1 and TUG1. (C) GC-1 spg cells were transfected with small interfering RNA (siRNA) targeting SRSF1 or scrambled control sequence (si NC). The expression of SRSF1 and clusterin were measured by real-time quantitative polymerase chain reaction (RT-qPCR). (D) GC-1 spg cells were transfected with vectors overexpressing TUG1 and siRNA targeting SRSF1 (or si NC). The expression of clusterin was measured by RT-qPCR. (E) GC-1 spg cells were transfected with vectors overexpressing TUG1 or control vectors. RIP was performed to verify the enrichment of clusterin by SRSF1. (F) The half-life of clusterin was determined by RNA stability assay. IgG, immunoglobulin G; GAPDH, glyceraldehyde-3-phosphate dehydrogenase; ActD, actinomycin D. $^{a}P<0.05$, $^{b}P<0.01$, $^{c}P<0.001$.

knockdown eliminated the effect of METTL3 overexpression on the apoptosis rate, and apoptosis-related proteins (Bcl-2, Bax, cleaved caspase-3, and cleaved caspase-9) of HG-stimulated GC-1 spg cells (Fig. 5I and J). Hence, it could be concluded that METTL3 regulated the viability and apoptosis of HG-stimulated GC-1 spg cells partly dependent on TUG1.

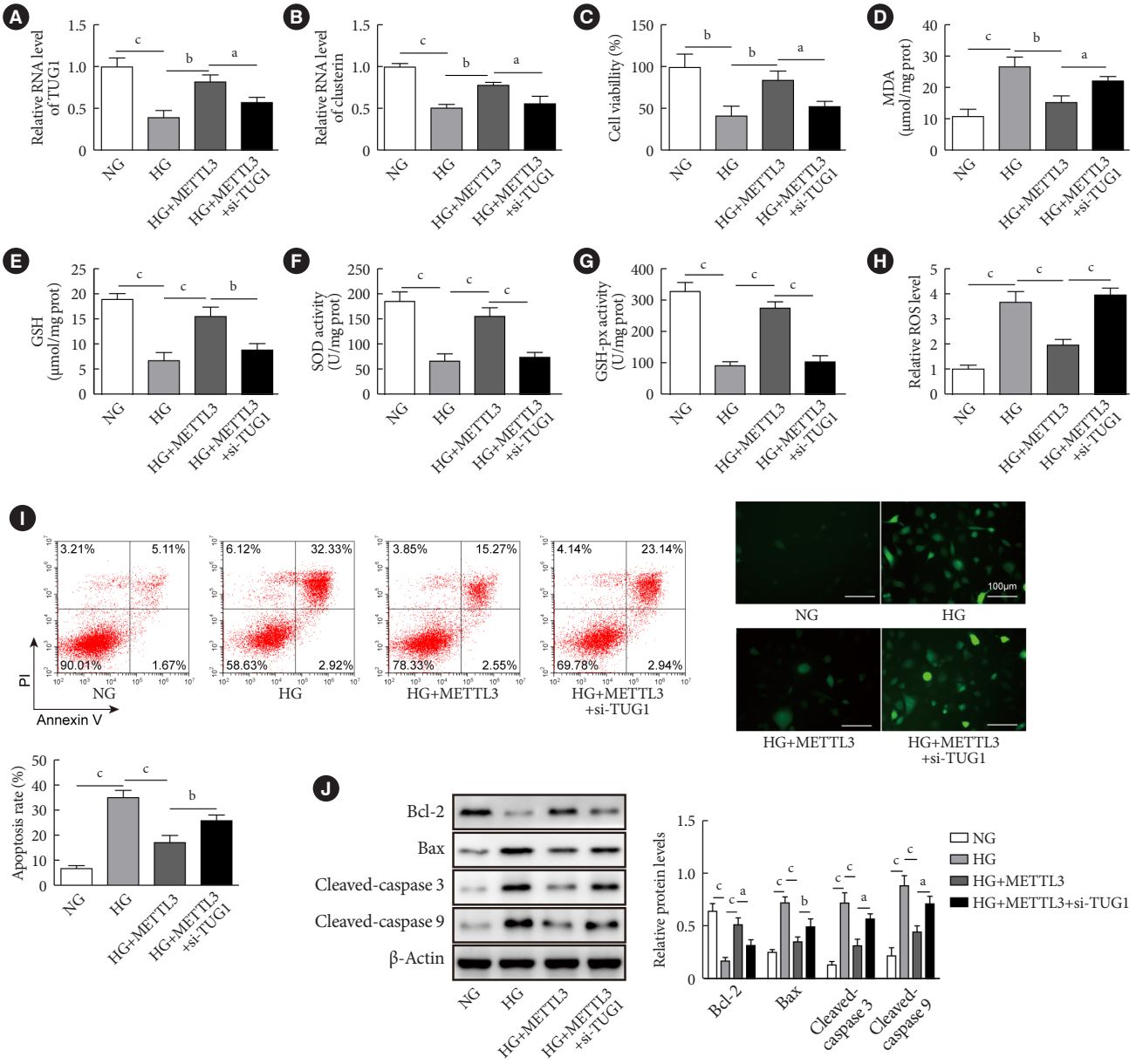

Fig. 5. Methyltransferase like-3 (METTL3) regulated the viability and apoptosis of high glucose (HG)-induced GC-1 spg cells via taurine up-regulated 1 (TUG1). GC-1 spg cells were co-transfected with pcDNA3.1-METTL3 vector and si TUG1 for 48 hours. Then, cells were exposed to HG conditions for 24 hours. (A, B) The RNA expressions of TUG1 and clustern were verified by real-time quantitative polymerase chain reaction. (C) Cell viability was evaluated by the MTT assay. (D, E, F, G) The levels of malondialdehyde (MDA) and glutathione (GSH) and the activities of superoxide dismutase (SOD) and glutathione peroxidase (GSH-Px) in GC-1 spg cells treated with or without HG were measured by commercial kits. (H) The level of reactive oxygen species (ROS) was detected using the 2′,7′-dichlorodihydro-fluorescin diacetate (DCFH-AD) probe. (I) Cell apoptosis was assessed by flow cytometry. (J) The expressions of Bcl-2, Bax, cleaved caspase-3, and cleaved caspase-9 were quantified by Western blot. NG, normal glucose. $^{a}P<0.05$, $^{b}P<0.01$, $^{c}P<0.001$.

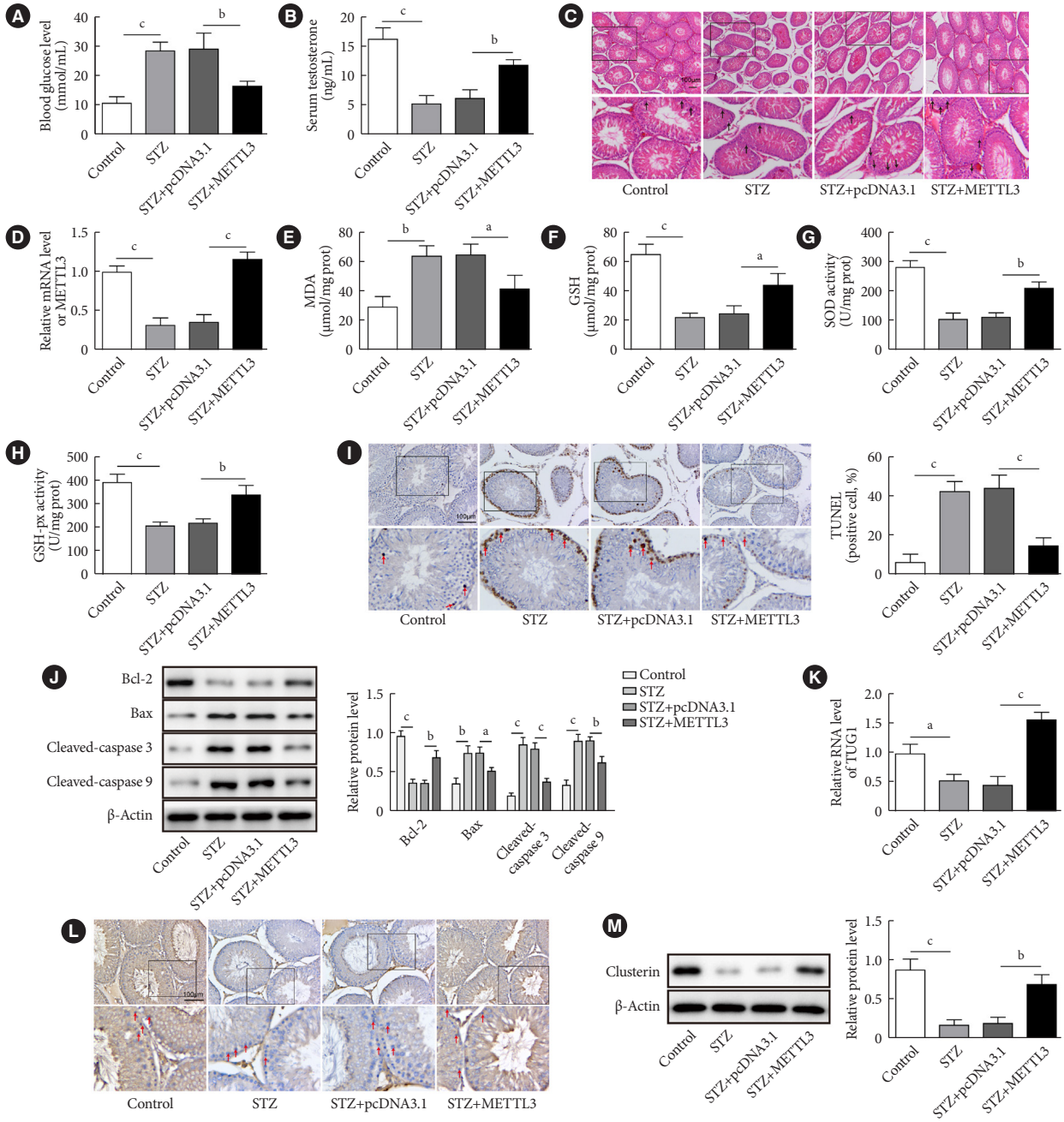

Fig. 6. Methyltransferase like-3 (METTL3) alleviated diabetes-induced testicular damage *in vivo*. The diabetic mice were then divided into three groups ($n=10$ per group): streptozocin (STZ), STZ+pcDNA3.1, and STZ+METTL3. After treatment, the testicular tissues and blood samples were collected for further detection. (A) The blood glucose level of STZ-treated mice and control mice was measured using a glucometer. (B) The serum level of testosterone was determined by enzyme-linked immunosorbent assay (ELISA). (C) H&E staining was performed to show pathophysiological changes in the testicles. (D) The expression of METTL3 was detected by real-time quantitative polymerase chain reaction (RT-qPCR). (D, E, F, G, H) The levels of malondialdehyde (MDA) and glutathione (GSH) and the activities of superoxide dismutase (SOD) and glutathione peroxidase (GSH-Px) in mouse testicular tissues were measured by commercial kits. (I) Terminal deoxynucleotidyl transferase dUTP nick end labeling (TUNEL) assay was performed to determine the apoptosis of cells in testicular tissues. (J) The expressions of Bcl-2, Bax, cleaved caspase-3, and cleaved caspase-9 were quantified by Western blot. (K) The RNA expression of taurine up-regulated 1 (TUG1) was assessed by RT-qPCR. (L, M) The protein expression of clusterin was measured by immunohistochemistry (IHC) and Western blot. $^{a}P<0.05$, $^{b}P<0.01$, $^{c}P<0.001$.

METTL3 alleviated DITD *in vivo*

Finally, the biological role of METTL3 in DITD *in vivo* was explored. As our observed, STZ treatment significantly elevated the blood glucose level and reduced testosterone level in mice, while these trend was greatly relieved by METTL3 overexpression (Fig. 6A and B). H&E staining disclosed that STZ injection led to severe injury of testicles, including decreased number of cells in the seminiferous tubule, disordered spermatozoa cells, and vacuolation of the cytoplasm; however, these pathological changes were notably alleviated by METTL3 overexpression (Fig. 6C). RT-qPCR detection showed that the injection of adenovirus-packaged METTL3-overexpressing vectors upregulated METTL3 expression (Fig. 6D). METTL3 overexpression significantly suppressed the level of MDA but enhanced the activities of SOD, GSH, and GSH-Px in testicular tissue of diabetic mice (Fig. 6E-H). The percentage of TUNEL-positive cells in testicular tissues was markedly elevated in diabetic mice, whereas METTL3 overexpression significantly reduced TUNEL-stained cells in the testicles (Fig. 6I). Consistently, the protein level of Bcl-2 was decreased while the expressions of Bax, cleaved caspase 3, and cleaved caspase 9 were upregulated in the testicular tissues of diabetic mice; however, METTL3 overexpression largely reversed these changes (Fig. 6J). In addition, METTL3 overexpression restored the RNA expression of TUG1 in the testicular tissues of diabetic mice (Fig. 6K). Downregulated expression of clusterin in the testicular tissues of diabetic mice was also markedly recovered by METTL3 overexpression (Fig. 6L and M). Comprehensively, our data demonstrated that METTL3 alleviated DITD *in vivo*.

DISCUSSION

Dynamic m6A modification is known to affect the development of diabetes and its related complications. The m6A mediators are abundantly expressed in human pancreatic β-cells and play a key regulatory role in cell cycle progression and insulin secretion of β-cells in type 2 diabetes mellitus [22]. METLL14, an m6A methyltransferase, regulated the survival, insulin secretion, and glucose metabolism of β-cells [23]. WTAP, another methyltransferase, was also proved to regulate adipogenesis and insulin sensitivity in mice [24]. A recent study by Li et al. [25] revealed that both the m6A level and METTL3 expression were increased in the livers of mice with hepatogenous diabetes and the overexpression of METTL3 aggravated high fat diet-induced insulin resistance and liver metabolic disorder. METTL3 have also been identified to mediate the fate determination of spermatogonial stem and progenitor cells [26,27]. Therefore, it is worthy to explore the regulatory potential of METTL3 in diseases associated with testicular dysfunction and fertility. In the present study, our data showed that METTL3 was downregulated in a mouse model of STZ-induced diabetes and mouse GC-1 spg cells exposed to HG. Moreover, overexpression of METTL3 notably attenuated the apoptosis of GC-1 spg cells and alleviated diabetes-induced pathological changes in the testicular tissues of mice. METTL3 has been considered a negative regulator of oxidative stress in colistin-induced kidney injury [28]. Also, it is believed that the downregulation of METTL3 in diabetes is related to oxidative conditions [29]. Here, we showed that METTL3 overexpression effectively protected against oxidative stress in HG-treated GC-1 spg cells and diabetic mice. Notably, the *in vivo* experiments described that the serum blood glucose level was greatly decreased after METTL3 overexpression. It has revealed that the improved blood glucose could modulate *in vivo* phenotypes [30]. Adenovirus METTL3 overexpression vector was injected intravenously into mice, and its overexpression effect was systemic, possibly affecting other sites except testicular tissue. Unfortunately, there seems to be no suitable way to rule out the effect of blood glucose levels on our study. Thus, we believe that adenovirus METTL3 overexpressed vector may affect the blood glucose level of diabetic mice by acting on liver, pancreas and other tissues and organs. From these above findings, it suggested that METTL3 might simultaneously alleviate testicular injury by affecting blood glucose level in mice or by inhibiting oxidative stress in testicular tissue.

As a key mediator of m6A, METTL3-mediated m6A modification has been widely reported to enhance the stability of target RNAs. Yue et al. [31] found that METTL3 regulated the epithelial-mesenchymal transition and metastasis of gastric cancer by increasing the stability of zinc finger MYM-type containing 1. Change et al. [32] demonstrated that METTL3 promoted the malignant progression of glioma by enhancing the stability of MALAT1 via m6A modification. In this study, we showed that METTL3-mediated m6A modification increased the stability of TUG1 in mouse spg cells. Notably, the functional role of TUG1 in diabetes is controversial. For instance, overexpression TUG1 could reverse the development of diabetes through reduced weight, blood glucose and insulin levels and testicular fat in diabetic mice [33]. It also exerted a protective role of TUG1 in both diabetic nephropathy and diabetes-induced endothelial progenitor cell dysfunction [12,13]. On the contrary, Yan et al.

[34] reported that TUG1 promoted the progression of diabetic atherosclerosis by regulating the Wnt signaling. Also, inhibition of TUG1 protected mice with diabetic cardiomyopathy against diastolic dysfunction [35]. Here, we showed that TUG1 was downregulated in diabetic mice and HG-stimulated GC-1 spg cells, and knockdown of TUG1 accelerated oxidative injury and cell apoptosis of HG-induced GC-1 spg cells, which greatly reversed the protective roles of METTL3 overexpression. These findings suggested that TUG1 might exert different effects in different diabetic complications.

The interaction between lncRNAs and RNA binding proteins (RBPs) is highly involved in the pathogenesis of diabetes-related disorders [36]. For example, lncRNA Blnc1 was found to protect against diet-induced obesity by activating the expression of RBP peroxisome proliferator-activated receptor gamma coactivator 1 [37]. SRSF1 is an RBP implicated in lncRNA MALAT1-mediated diabetic nephropathy and HG-induced podocyte injury [38]. Here, our data described that found that TUG1 interacted with SRSF1 to stabilize clusterin mRNA in GC-1 spg cells. Clusterin is a key apoptosis regulatory that has been found to mediate fluorosis-induced GC-1 spg cell apoptosis [39]. Our previous study further showed that clusterin overexpression suppressed autophagy-mediated apoptosis of GC-1 spg cells by activating the PI3K/Akt/mTOR signaling pathway [17]. Moreover, clusterin has been identified as a sensor of oxidative stress in diabetics [40]. Consistent to previous work, our experimental data demonstrated that clusterin mRNA could be stabilized by TUG1 overexpression via recruiting SRSF1. Moreover, we also highlighted that clusterin was increased in diabetic mice after METTL3 overexpression. These results implied the potential correlation among clusterin, TUG1, and METTL3, revealing TUG1/clusterin was the downregulation effective mechanism of METTL3 in DITD.

In conclusion, our study revealed that overexpression of METTL3 alleviated HG-triggered oxidative damage and apoptosis of spermatogenic cells by elevating m6A modification of TUG1, thus promoting SRSF1-stabilized clusterin mRNA stability, which further elucidated the underlying mechanisms of DITD, and also indicated that METTL3 might be a therapeutic molecular in DITD.

CONFLICTS OF INTEREST

No potential conflict of interest relevant to this article was reported.

AUTHOR CONTRIBUTIONS

Conception or design: Y.T., F.S.
Acquisition, analysis, or interpretation of data: Y.H.X., C.S., BL.
Drafting the work or revising: Y.T., F.S.
Final approval of the manuscript: Y.T., Y.H.X., C.S., BL., F.S.

ORCID

Yuan Tian *https://orcid.org/0000-0002-5291-3202*
Fa Sun *https://orcid.org/0000-0002-0841-4668*

FUNDING

This work was supported by Guizhou Provincial High-level Innovative Talents "Hundred level" Guizhou Science Cooperation Platform Talents (2016) (No. 4017); Guizhou Provincial Science and Technology Planning Project Qkehezui (2020) (No. 4y142); Guizhou Urology Graduate Workstation (No. qkyh gzz [2016] 04); Science and Technology Project of Guizhou Provincial Health Commission (No. gzwjkj-2018-1-037); Science and Technology Project Zhuke Contract of Guiyang science and Technology Bureau (2019) (No. 9-1-17). The funders had no role in study design, data collection and analysis, decision to publish, or preparation of the manuscript.

ACKNOWLEDGMENTS

None

REFERENCES

1. Liu Y, Yang Z, Kong D, Zhang Y, Yu W, Zha W. Metformin ameliorates testicular damage in male mice with streptozotocin-induced type 1 diabetes through the PK2/PKR pathway. Oxid Med Cell Longev 2019;2019:5681701.
2. Ghazi S, Zohdy W, Elkhiat Y, Shamloul R. Serum testosterone levels in diabetic men with and without erectile dysfunction. Andrologia 2012;44:373-80.
3. Agbaje IM, Rogers DA, McVicar CM, McClure N, Atkinson AB, Mallidis C, et al. Insulin dependant diabetes mellitus: implications for male reproductive function. Hum Reprod 2007; 22:1871-7.
4. Long L, Qiu H, Cai B, Chen N, Lu X, Zheng S, et al. Hyperglycemia induced testicular damage in type 2 diabetes mellitus

rats exhibiting microcirculation impairments associated with vascular endothelial growth factor decreased via PI3K/Akt pathway. Oncotarget 2018;9:5321-36.
5. Zhao Y, Chen Y, Jin M, Wang J. The crosstalk between m6A RNA methylation and other epigenetic regulators: a novel perspective in epigenetic remodeling. Theranostics 2021;11:4549-66.
6. Jiang X, Liu B, Nie Z, Duan L, Xiong Q, Jin Z, et al. The role of m6A modification in the biological functions and diseases. Signal Transduct Target Ther 2021;6:74.
7. Huang H, Weng H, Chen J. m6A modification in coding and non-coding RNAs: roles and therapeutic implications in cancer. Cancer Cell 2020;37:270-88.
8. Yang J, Liu J, Zhao S, Tian F. N(6)-Methyladenosine METTL3 modulates the proliferation and apoptosis of lens epithelial cells in diabetic cataract. Mol Ther Nucleic Acids 2020;20:111-6.
9. Zha X, Xi X, Fan X, Ma M, Zhang Y, Yang Y. Overexpression of METTL3 attenuates high-glucose induced RPE cell pyroptosis by regulating miR-25-3p/PTEN/Akt signaling cascade through DGCR8. Aging (Albany NY) 2020;12:8137-50.
10. Liu JY, Yao J, Li XM, Song YC, Wang XQ, Li YJ, et al. Pathogenic role of lncRNA-MALAT1 in endothelial cell dysfunction in diabetes mellitus. Cell Death Dis 2014;5:e1506.
11. Yang F, Qin Y, Wang Y, Li A, Lv J, Sun X, et al. LncRNA KCNQ1OT1 mediates pyroptosis in diabetic cardiomyopathy. Cell Physiol Biochem 2018;50:1230-44.
12. Long J, Badal SS, Ye Z, Wang Y, Ayanga BA, Galvan DL, et al. Long noncoding RNA Tug1 regulates mitochondrial bioenergetics in diabetic nephropathy. J Clin Invest 2016;126:4205-18.
13. Li Y, Zhi K, Han S, Li X, Li M, Lian W, et al. TUG1 enhances high glucose-impaired endothelial progenitor cell function via miR-29c-3p/PDGF-BB/Wnt signaling. Stem Cell Res Ther 2020;11:441.
14. Wilson MR, Zoubeidi A. Clusterin as a therapeutic target. Expert Opin Ther Targets 2017;21:201-13.
15. Ren L, Han F, Xuan L, Lv Y, Gong L, Yan Y, et al. Clusterin ameliorates endothelial dysfunction in diabetes by suppressing mitochondrial fragmentation. Free Radic Biol Med 2019;145:357-73.
16. He J, Dijkstra KL, Bakker K, Bus P, Bruijn JA, Scharpfenecker M, et al. Glomerular clusterin expression is increased in diabetic nephropathy and protects against oxidative stress-induced apoptosis in podocytes. Sci Rep 2020;10:14888.
17. Tian Y, Xiao YH, Geng T, Sun C, Gu J, Tang KF, et al. Clusterin suppresses spermatogenic cell apoptosis to alleviate diabetes-induced testicular damage by inhibiting autophagy via the PI3K/AKT/mTOR axis. Biol Cell 2021;113:14-27.
18. Verma P, Parte P. Revisiting the characteristics of testicular germ cell lines GC-1(spg) and GC-2(spd)ts. Mol Biotechnol 2021;63:941-52.
19. Zheng H, Huang J, Zhang M, Zhao HJ, Chen P, Zeng ZH. miR-27b-3p improved high glucose-induced spermatogenic cell damage via regulating Gfpt1/HBP signaling. Eur Surg Res 2022;63:64-76.
20. Liao J, Xiao H, Dai G, He T, Huang W. Recombinant adenovirus (AdEasy system) mediated exogenous expression of long non-coding RNA H19 (lncRNA H19) biphasic regulating osteogenic differentiation of mesenchymal stem cells (MSCs). Am J Transl Res 2020;12:1700-13.
21. Rastogi RP, Singh SP, Hader DP, Sinha RP. Detection of reactive oxygen species (ROS) by the oxidant-sensing probe 2',7'-dichlorodihydrofluorescein diacetate in the cyanobacterium Anabaena variabilis PCC 7937. Biochem Biophys Res Commun 2010;397:603-7.
22. De Jesus DF, Zhang Z, Kahraman S, Brown NK, Chen M, Hu J, et al. m6A mRNA methylation regulates human β-cell biology in physiological states and in type 2 diabetes. Nat Metab 2019;1:765-74.
23. Liu J, Luo G, Sun J, Men L, Ye H, He C, et al. METTL14 is essential for β-cell survival and insulin secretion. Biochim Biophys Acta Mol Basis Dis 2019;1865:2138-48.
24. Kobayashi M, Ohsugi M, Sasako T, Awazawa M, Umehara T, Iwane A, et al. The RNA methyltransferase complex of WTAP, METTL3, and METTL14 regulates mitotic clonal expansion in adipogenesis. Mol Cell Biol 2018;38:e00116-18.
25. Li Y, Zhang Q, Cui G, Zhao F, Tian X, Sun BF, et al. m6A regulates liver metabolic disorders and hepatogenous diabetes. Genomics Proteomics Bioinformatics 2020;18:371-83.
26. Lin Z, Hsu PJ, Xing X, Fang J, Lu Z, Zou Q, et al. Mettl3-/Mettl14-mediated mRNA N6-methyladenosine modulates murine spermatogenesis. Cell Res 2017;27:1216-30.
27. Zhang C, Chen Y, Sun B, Wang L, Yang Y, Ma D, et al. m6A modulates haematopoietic stem and progenitor cell specification. Nature 2017;549:273-6.
28. Wang J, Ishfaq M, Xu L, Xia C, Chen C, Li J. METTL3/m6A/miRNA-873-5p attenuated oxidative stress and apoptosis in colistin-induced kidney injury by modulating Keap1/Nrf2 pathway. Front Pharmacol 2019;10:517.
29. Li X, Jiang Y, Sun X, Wu Y, Chen Z. METTL3 is required for

maintaining β-cell function. Metabolism 2021;116:154702.
30. Kapucu A, Akgun-Dar K. Leptin ameliorates testicular injury by altering expression of nitric oxide synthases in diabetic rats. Bratisl Lek Listy 2021;122:111-5.
31. Yue B, Song C, Yang L, Cui R, Cheng X, Zhang Z, et al. METTL3-mediated N6-methyladenosine modification is critical for epithelial-mesenchymal transition and metastasis of gastric cancer. Mol Cancer 2019;18:142.
32. Chang YZ, Chai RC, Pang B, Chang X, An SY, Zhang KN, et al. METTL3 enhances the stability of MALAT1 with the assistance of HuR via m6A modification and activates NF-κB to promote the malignant progression of IDH-wildtype glioma. Cancer Lett 2021;511:36-46.
33. Zhang Y, Ma Y, Gu M, Peng Y. lncRNA TUG1 promotes the brown remodeling of white adipose tissue by regulating miR-204-targeted SIRT1 in diabetic mice. Int J Mol Med 2020;46:2225-34.
34. Yan HY, Bu SZ, Zhou WB, Mai YF. TUG1 promotes diabetic atherosclerosis by regulating proliferation of endothelial cells via Wnt pathway. Eur Rev Med Pharmacol Sci 2018;22:6922-9.
35. Zhao L, Li W, Zhao H. Inhibition of long non-coding RNA TUG1 protects against diabetic cardiomyopathy induced diastolic dysfunction by regulating miR-499-5p. Am J Transl Res 2020;12:718-30.
36. Kim C, Kang D, Lee EK, Lee JS. Long noncoding RNAs and RNA-binding proteins in oxidative stress, cellular senescence, and age-related diseases. Oxid Med Cell Longev 2017;2017:2062384.
37. Tang S, Zhu W, Zheng F, Gui W, Zhang W, Lin X, et al. The long noncoding RNA Blnc1 protects against diet-induced obesity by promoting mitochondrial function in white fat. Diabetes Metab Syndr Obes 2020;13:1189-201.
38. Hu M, Wang R, Li X, Fan M, Lin J, Zhen J, et al. LncRNA MALAT1 is dysregulated in diabetic nephropathy and involved in high glucose-induced podocyte injury via its interplay with β-catenin. J Cell Mol Med 2017;21:2732-47.
39. Tian Y, Xiao Y, Wang B, Sun C, Tang K, Sun F. Vitamin E and lycopene reduce coal burning fluorosis-induced spermatogenic cell apoptosis via oxidative stress-mediated JNK and ERK signaling pathways. Biosci Rep 2018;38:BSR20171003.
40. Wittwer J, Bradley D. Clusterin and its role in insulin resistance and the cardiometabolic syndrome. Front Immunol 2021;12:612496.